CrossMark

Surface Chemistry and Flotation Behaviors of Monazite–Apatite–Ilmenite–Quartz–Rutile–Zircon with Octanohydroxamic Acid

J. Nduwa-Mushidi[1], ⬤ · C. G. Anderson[1],

Abstract Global demand and consumption of rare earth elements and compounds have led to increasing research to further our understanding of their beneficiation and recovery. Monazite is the second-most important rare earth-bearing mineral that can be exploited. In this study, the surface chemistry of monazite in terms of zeta potential, adsorption density, and flotation responses using octanohydroxamic acid is determined. Apatite, ilmenite, quartz, rutile, and zircon are the minerals that frequently occur with monazite, and hence they were chosen as gangue minerals in this study. The isoelectric points of monazite, apatite, ilmenite, quartz, rutile, and zircon are 5.3, 8.7, 3.8, 3.4, 6.3, and 5.1, respectively. Thermodynamic parameters of adsorption were evaluated. Ilmenite has the highest driving force for adsorption. Adsorption density value shows that octanohydroxamic acid adsorbs onto monazite and its gangue minerals. This observation was further confirmed by microflotation experiments. Increasing the temperature to 80 °C raises the adsorption and floatability of monazite and gangue minerals, which does not allow for separation. Monazite is best recovered at a pH range of 7.5–10. Appropriate use of depressant is recommended in order to enhance the separation of monazite from its gangue.

Keywords Rare-earth · Beneficiation · Flotation · Monazite · Heavy mineral sand

✉ J. Nduwa-Mushidi
  josuenduwa@gmail.com

[1] Kroll Institute of Extractive Metallurgy, Critical Materials Institute, Colorado School of Mines, Golden, CO 80401, USA

Introduction

Increase in technological advancement has led to an enhancement in global demand for rare earth metals and compounds. Despite their name implying so, rare earth elements, however, are abundant in the earth's crust; however, their concentrations in most places are relatively too low to allow for an efficient metallurgical extraction. The main deposits of rare earth minerals are located in China, the United States, Australia, Canada, Brazil, and distributed across various countries in Central Africa.

Monazite is the second-most important source of rare earths, after bastnaesite. Monazite is a rare earth phosphate mineral that contains various amounts of thorium. Originally, monazite was the primary source of rare earth elements as byproducts of the production of thorium and uranium. Thorium was viewed as a possible fuel for nuclear reactors. The decreasing interest in thorium due to environmental concerns shifted the importance of monazite toward the extraction of rare earth elements by established metallurgical processes. The most important sources of monazite are placer deposits that are easy to mine. Monazite often accumulates with other minerals such as ilmenite, rutile, zircon, quartz, magnetite, and sometimes gold.

Due to its relatively high specific gravity (4.9–5.5), monazite is beneficiated along with other heavy minerals by means of gravity separation. Monazite is further separated from other heavy minerals by a series of magnetic and electrostatic separation processes. However, these physical methods of separation become less efficient when the size of the liberated particle gets smaller. In the latter case, efficient separation can be achieved by flotation.

The literature on the flotation of monazite is rather scarce. The available literature focuses on the separation of monazite from xenotime, bastnaesite, rutile, and zircon.

The floatability behavior of monazite is very similar to that of its associated minerals, and thus is a challenge to separate. This can be seen in the work done by Pavez and Peres in a system of monazite–rutile–zircon using sodium oleate and hydroxamates [1], by Ren in a system of monazite–bastnaesite using benzoic acid [2], by McEwen in a system of monazite–feldspar–ilmenite–rutile–garnet–zircon using amine acetate and sodium petroleum sulfonate [3], and by Abeidu in a system of monazite–zircon using oleic acid [4].

There is a wide range of reported isoelectric point (IEP) for monazite. Cheng reported IEP values ranging from 1.1 to 9 [5]. However, most values reported in the literature fall within the range from 5.0 to 6.4. The differences in IEP values may be attributed to impurities and differences in mineral composition and/or in experimental methods, and to radiation damage of the lattice caused by the presence of thorium.

Very little is known about adsorption density values of different collectors onto the surface of monazite. Only a few studies have been conducted on adsorption density on monazite with an oleate collector [6–8].

Hydroxamic acid, which may be considered as a derivative of hydroxyl amine and carboxyl acid, adsorbs onto mineral surfaces by a chelating reaction as shown in Fig. 1 [9].

In this study, apatite, ilmenite, quartz, rutile, and zircon were chosen as associated minerals due to their occurrence with monazite in mineral deposits. The separation by flotation of monazite from these minerals relies on the difference in the surface chemistry profile of the minerals.

Understanding the surface properties of these minerals is the basis for establishing the concentration of monazite and, ultimately, improving the production of rare earth elements and compounds.

This study presents the surface chemistry profiles and flotation behaviors of monazite and associated minerals in terms of zeta potential measurements, adsorption density, and microflotation experiments. Thermodynamic data, calculated from adsorption studies, are also presented in this paper. The experimental procedures used in this study are similar to that of Pradip's on bastnaesite, barite, and calcite [10].

Materials and Methods

Minerals and Reagents

A high-purity monazite mineral was obtained from Persson Rare Minerals. The sample originated from New Mexico. The composition and mineralogy of the sample were confirmed by Mineral Liberation Analysis (MLA) and X-Ray Diffraction (XRD) analyses performed at Montana Tech Camp. XRD results reported 100% purity for monazite,

while the MLA revealed 97.6% purity, with other minerals such as 0.72% auerlite $(Th_{0.8},Ca_{0.2})(VO_4,SiO_4,PO_4)$.

High-purity apatite (fluorapatite), ilmenite, and quartz samples were obtained from Van Waters and Rogers (VWR). The purity of samples was determined by X-Ray Fluorescent (XRF) and XRD. Rutile and zircon samples were obtained from Excalibur Mineral Corp. The samples were also confirmed by XRF and XRD.

Research grade octanohydroxamic acid $(C_8H_{17}NO_2)$ was obtained from Tokyo Chemical Industry Co., Ltd (TCI).

Experimental Procedures

Zeta Potential

The zeta potential of each mineral was evaluated as a function of pH by streaming potential method using a Stabino Particle Charge Mapping from Microtrac. Pulverized samples were added into aqueous suspensions in 50-mL polyethylene tubes, and conditioned on a shaking table for 24 h. Suspensions were 0.05% solid. 0.1 N solutions of both HCl and NaOH were used as pH modifiers throughout zeta potential measurements.

Effects of cerium- and phosphate-determining ions on the zeta potential of monazite were evaluated. A series of experiments were also conducted to determine the effect of octanohydroxamic acid on the zeta potential of each mineral.

Adsorption Density

The adsorption of octanohydroxamic acid on the surface of each mineral was evaluated by the solution depletion method; the concentrations of hydroxamic acid are measured before and after adsorption. The difference was assumed to be due to adsorption onto the surface. The adsorption density was calculated according to the following equation:

$$\Gamma_\delta = \frac{\Delta C V}{mA},$$

where ΔC is the change in molar concentration of the solution before and after adsorption, V is the volume of hydroxamic acid solution in liters, m is the mass of solid used in grams, and A is the specific area in m^2/g.

Predetermined amounts of solid minerals were mixed with a known concentration of hydroxamic acid. Each suspension was shaken at the temperature of experiment until equilibrium was reached. The mixture was then centrifuged to separate the solid from the liquid; the latter is needed to determine the concentration.
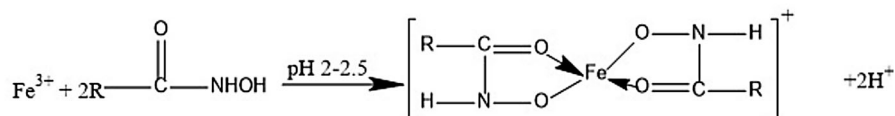
The concentration of the liquid was evaluated by colorimetry using a UV–Visible spectrophotometer; hydroxamic acid forms a complex with ferric perchloride. The
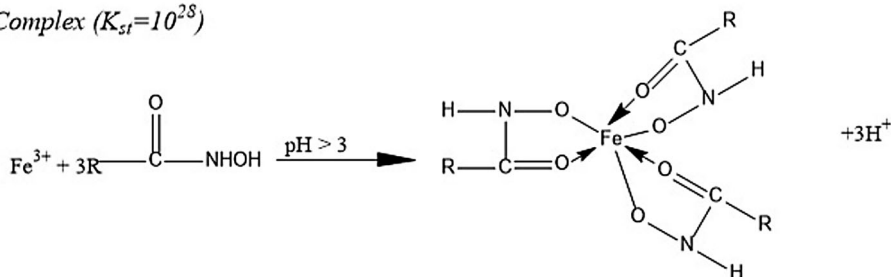
Fig. 1 Formation of ferric hydroxamate complexes [9]

1:1 Complex ($K_{st}=10^{11}$)
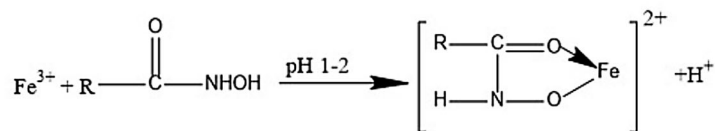
1:2 Complex ($K_{st}=10^{30.5}$)

1:3 Complex ($K_{st}=10^{28}$)

ferric hydroxamate complex has a characteristic peak detectable by the spectrophotometer at 500 nm.

The surface area of solid minerals was evaluated by Brunauer-Emmett-Teller (BET) method using nitrogen gas. Each mineral was grinded to −325 mesh.

Adsorption density experiments consisted of determining solid–liquid ratio, kinetics of adsorption, and adsorption isotherm. Each of these experiments was conducted for all minerals at room temperature and at 80 °C. In addition, the effect of pH on adsorption was evaluated at room temperature.

The free energy of adsorption was calculated at 25 and 80 °C using the Stern–Grahame equation [11]. Given the free energy at two different temperatures, the enthalpy and entropy of adsorption could also be calculated.

Microflotation

The floatability of each mineral was evaluated by microflotation experiment in a modified Hallimond tube. Half a gram of pure mineral was conditioned in a beaker on a stirring plate for 15 min in 55 mL of the collector solution at desired concentration and pH. The slurry was transferred into the Hallimond tube and stirred throughout the flotation experiment. Two-minute flotation tests were conducted by passing air through the tube at 60 cc/min.

High-temperature flotation tests were conducted by conditioning for 15 min at 80 °C prior to flotation. Careful measures were taken to prevent evaporation of the aqueous solution during conditioning.

The concentrate and tailing were filtered, dried, and weighed. The results were expressed on a weight basis (floatability).

Results and Discussion

Zeta Potential

Results in Fig. 2 show the zeta potential values of monazite, apatite, ilmenite, quartz, rutile, and zircon. The IEP values are 5.3, 8.7, 3.8, 3.4, 6.3, and 5.1, respectively. The zeta potential of monazite is negative at higher pH, and becomes more positive as the pH reaches lower values. The IEP of monazite is similar to that reported in the literature by Pavez and Peres [12], Cheng et al. [5], and Houlo et al. [13].

The IEPs of the other minerals have been reported in the literature: Apatite is reported at variant IEP values at pH 3.5, 5.5, 6.7 [14], pH 4.2 [15], and pH 7.5 [16]. The IEP of ilmenite found in this study (3.8) is lower than the values (4.2–6.25) found by Mehdilo [17]. The IEP of quartz is
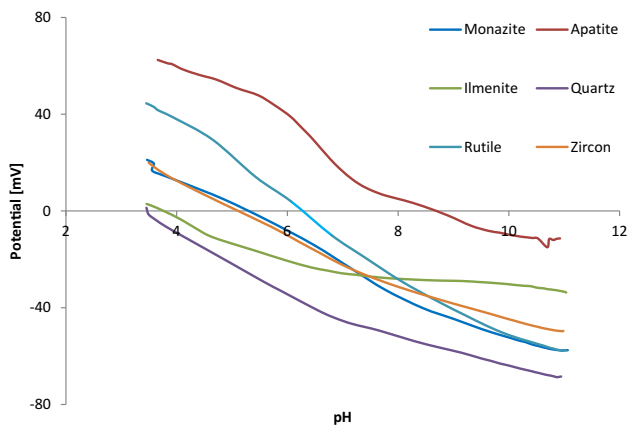
Fig. 2 Zeta potentials of monazite, apatite, ilmenite, quartz, rutile, and zircon as a function of pH in water (Color figure online)

higher than the value found by Zhou [18]. In another study, Zhou reported that the surface potential of quartz remained negative at all pH values. The literature value on the IEP of rutile is 4.5 [1].

The differences in reported IEP values may be due to impurities, differences in mineral composition, and in experimental methods, or to lattice damage caused by radiation due to the presence of thorium in the case of monazite.

The effects of cerium potential- and phosphate potential-determining ions are also investigated and presented in Fig. 3. As expected, the zeta potential of monazite shifts toward more positive values, and the IEP shifts to the right when monazite is in equilibrium with a cerium nitrate aqueous solution. This behavior results from the adsorption of cerium cations or cerium hydroxyl cations onto the surface of monazite, which renders the surface more positively charged. Similarly, the IEP shifts to the left with the addition of phosphate ions, and zeta potential remains negative in the range of pH of this experiment. Other rare earth ions, such as La^{3+}, Nd^{3+}, etc., may also be potential-determining ions. Their effects on the zeta potential of monazite are expected to be similar to that of cerium ions.

Figures 4, 5, 6, 7, 8, and 9 present the zeta potential of monazite and its associated minerals as a function of pH in 10^{-3} molar solutions of octanohydroxamic acid. For comparison, the zeta potential in water is also plotted. With the exception of quartz and ilmenite, the IEPs of minerals shift to the left with the addition of octanohydroxamic acid. Moreover, the octanohydroxamic acid has no effect on the zeta potential of quartz, which can be explained by the limited interaction of quartz and octanohydroxamic acid, as reflected in the adsorption density results.

The change in the zeta potential is an indication that octanohydroxamic acid collector adsorbs onto the surfaces of minerals.
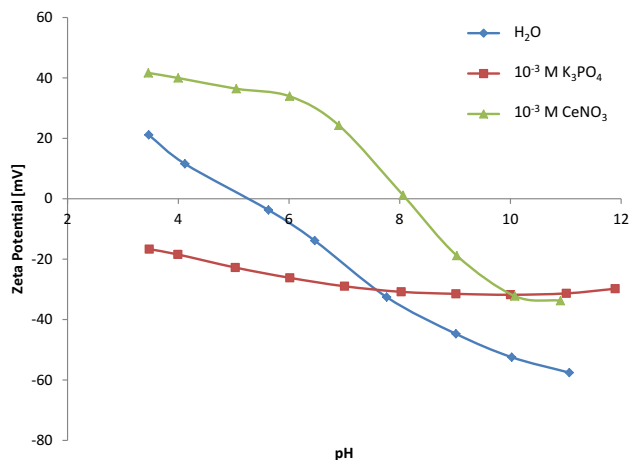

Fig. 3 Zeta potential of monazite as a function of pH in water, 10^{-3} M K_3PO_4, and 10^{-3} M $CeNO_3$
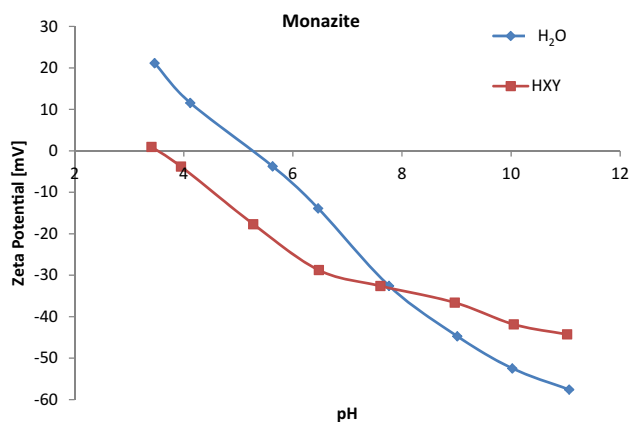

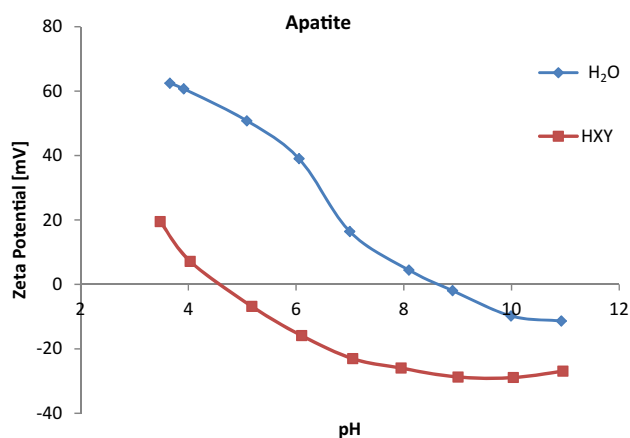**Fig. 4** Zeta potential of monazite in 10^{-3} M octanohydroxamic acid

Fig. 5 Zeta potential of apatite in 10^{-3} M octanohydroxamic acid

Adsorption occurs at pH lower than 9.5, which is the pK_a of hydroxamic acid [5]. In this range, octanohydroxamic acid molecules are predominant. This indicates that the octanohydroxamic acid molecule is the adsorbing
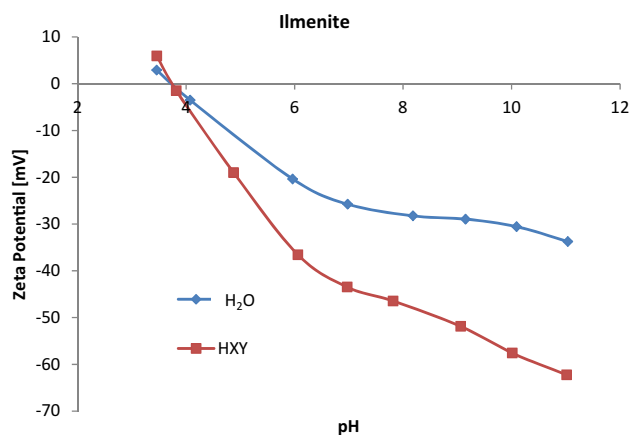
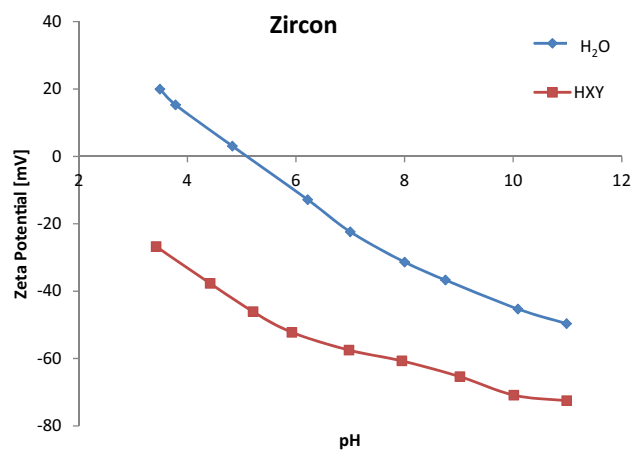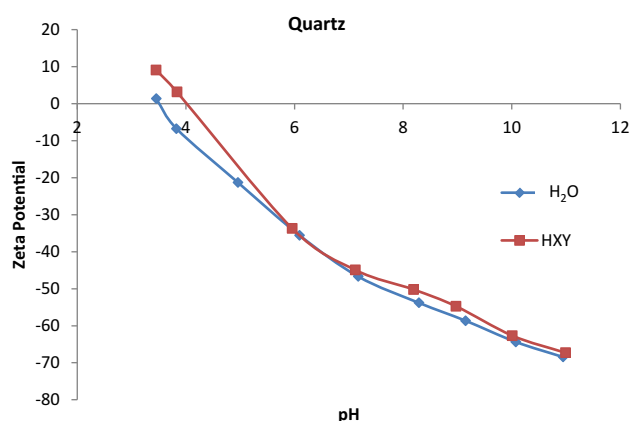Fig. 6 Zeta potential of ilmenite in 10^{-3} M octanohydroxamic acid

Fig. 7 Zeta potential of quartz in 10^{-3} M octanohydroxamic acid
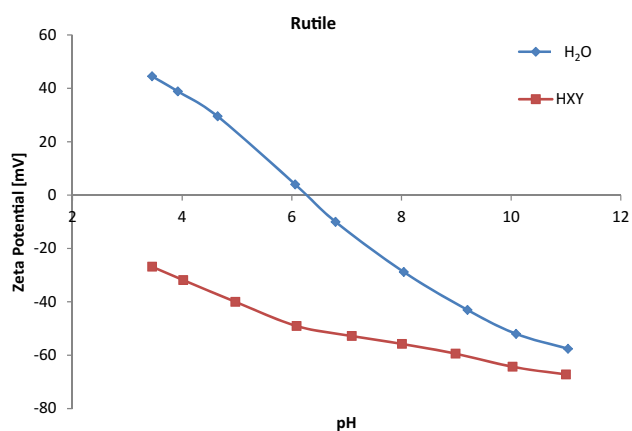

Fig. 8 Zeta potential of rutile in 10^{-3} M octanohydroxamic acid

agent. At higher pH, however, octanohydroxamate anion is responsible for adsorption.

Octanohydroxamic acid adsorbs on the surface of negatively charged particles. This is an indication that adsorption mechanism might be of chemical nature.

Fig. 9 Zeta potential of zircon in 10^{-3} M octanohydroxamic acid

Adsorption Density

In adsorption kinetic experiments, the adsorption density values were plotted as a function of time for monazite, apatite, ilmenite, quartz, rutile, and zircon. The initial concentration was 10^{-3} M for all kinetic experiments. The result is shown in Fig. 10. Twenty-four hours were found sufficient to reach equilibrium for apatite, 48 h for monazite, quartz, and rutile, and 96 h was sufficient for ilmenite and zircon. The following adsorption experiments at room temperature, including adsorption isotherm and effect of pH on adsorption, were carried using the resulted equilibrium times.

Similar experiments were performed at 80 °C. The resulting equilibrium times, as seen in Fig. 11, are 24 h for apatite and zircon, 60 h for ilmenite and quartz, and 90 h for monazite and rutile. These equilibrium times were used for subsequent adsorption experiments at 80 °C.

Due to its relatively elevated and fast solubility in water [19], apatite reaches equilibrium in much shorter time period.

Minerals are abbreviated as follows:

- Monazite: Mnz
- Apatite: Ap
- Ilmenite: Ilm
- Quartz: Qtz
- Rutile: Rt
- Zircon: Zrn

The abbreviations were adapted from Siivalo and Schmiid-published minerals abbreviation list [20].

It is important to note that initial concentrations have negligible effect on the equilibrium time in kinetics experiments. Figure 12 illustrates the kinetics of adsorption of monazite at initial concentrations of 10^{-3} M and 2×10^{-3} M octanohydroxamic acid. In both cases, the
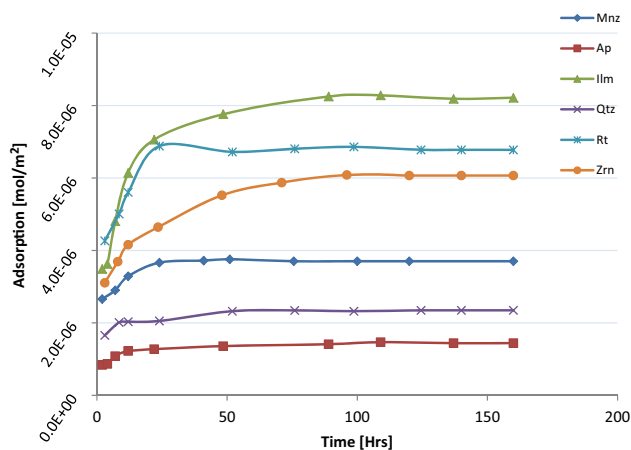
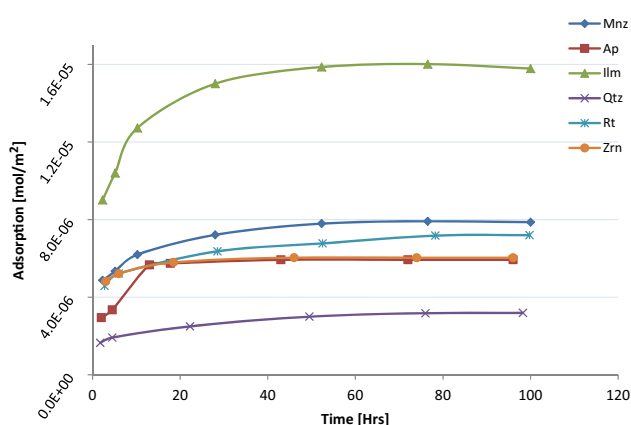**Fig. 10** Kinetics of adsorption at 25 °C

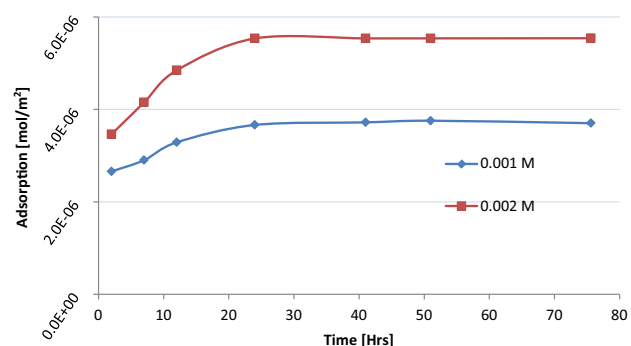**Fig. 11** Kinetics of adsorption at 80 °C

Fig. 12 Kinetics of adsorption of octanohydroxamic acid onto monazite at 25 °C, at initial concentrations of 10^{-3} and 2×10^{-3} M

equilibrium time is 24 h; however, higher degree of adsorption is observed at higher initial concentration.

Adsorption isotherm experiments were conducted to delineate the effect of equilibrium concentration and temperature on the adsorption density. Figure 13 presents the adsorption isotherm of monazite and associated minerals at room temperature (25 °C) and at 80 °C.

Assuming the vertical and horizontal cross-sectional areas of hydroxamate group to be 20.5 and 55 Å^2, respectively [10], the vertical and horizontal monolayer adsorption density values were calculated to be 8.1×10^{-6} and 3.02×10^{-6} mol/m^2, respectively. The vertical and horizontal monolayers of adsorption are represented in Fig. 13 by black and red horizontal dashed lines, respectively.

Ilmenite, rutile, and zircon experience higher adsorption density values at room temperature. The vertical monolayer coverage of octanohydroxamic acid on the surface of these minerals occurs at relatively low equilibrium concentration (2×10^{-3}–10^{-3} M) in the bulk solution. This indicates high driving forces of adsorption, and hence, high free energies of adsorption. Apatite has a medium adsorption level.

Apatite does not exhibit a plateau at either temperature. This continuously increasing adsorption density recorded for apatite may be due to bulk precipitation of octanohydroxamate with calcium ions in solution. Three types of interactions between collector and minerals can happen in chemisorption [21]: *Chemisorption* occurs during a monolayer adsorption by interaction between the collector and the surface without the movement of atoms from their lattice sites. *Surface reaction* happens by interaction with the movement of the lattice atoms, when multilayer adsorption occurs. *Bulk precipitation* occurs by reaction of the metal reagent and the collector away from the surface. This happens when the rate of dissolution is faster than the rate of reaction of collector and the lattice metal. In this adsorption density study, bulk precipitation could not be detected due to limitations of the solution depletion method; therefore, it would be interpreted as adsorption onto the surface.

The adsorption uptake of octanohydroxamic acid on monazite shows lower adsorption density. The plateau corresponding to monolayer adsorption occurs at 6 ± 0.2 μmol/m^2.

Quartz shows the lowest adsorption density among the minerals under investigation in this study. The adsorption on quartz does not reach vertical monolayer coverage, which indicates that octanohydroxamic acid adsorbs onto the surface of quartz in a horizontal configuration.

Temperature has remarkable effects on the adsorption density, with the exception of quartz, which shows limited temperature dependency on adsorption. As opposed to the other minerals, increasing temperature results in a decrease in adsorption density on quartz mineral.

Increasing the temperature from 25 to 80 °C leads to an increase in adsorption density on the surface of monazite by a factor of 3.5. This temperature dependency indicates a higher entropy of adsorption as it is observed from the thermodynamics calculations. It is well known that the
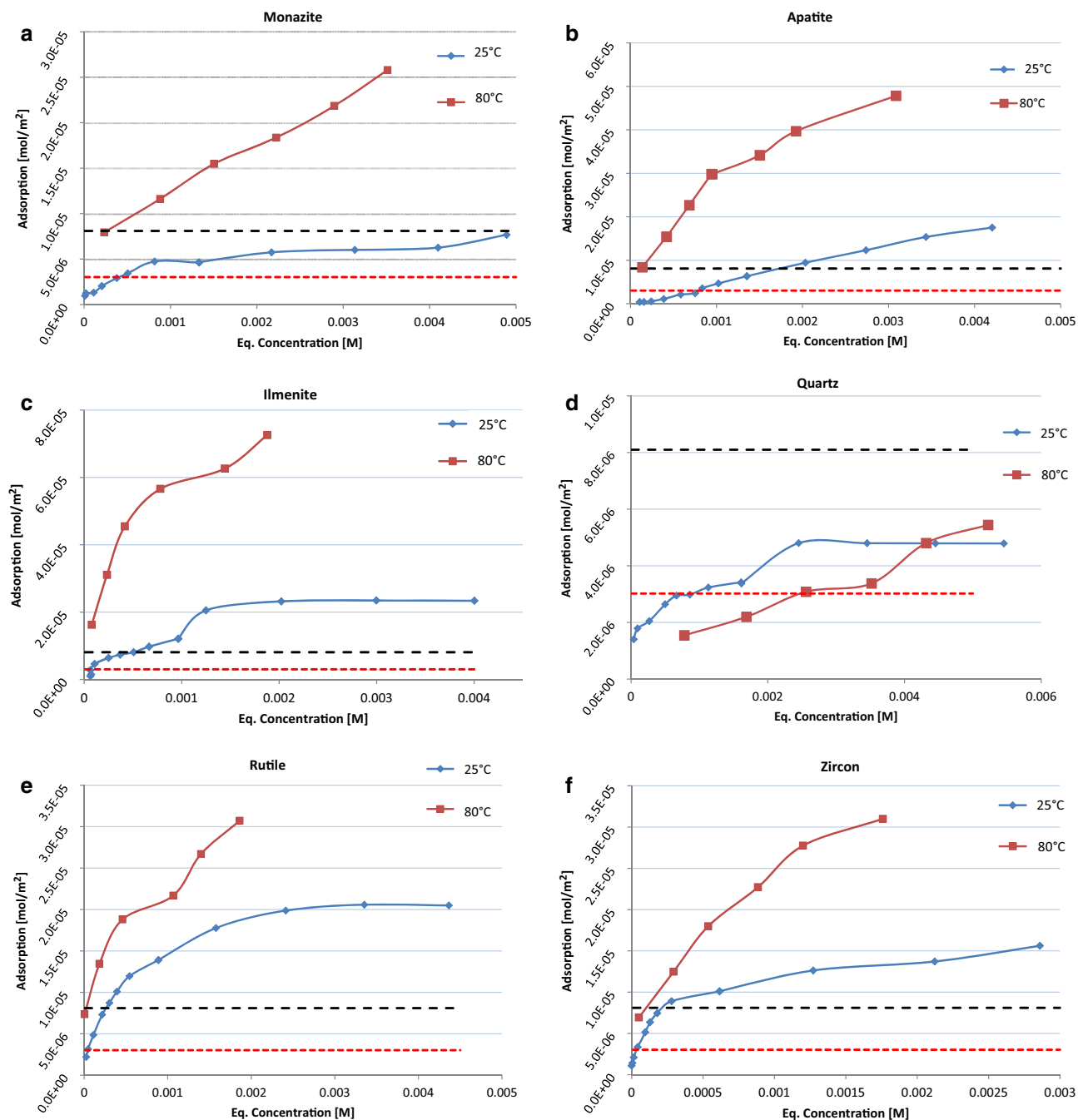
Fig. 13 Adsorption isotherms of octanohydroxamic acid onto **a** monazite, **b** apatite, **c** ilmenite, **d** quartz, **e** rutile, and **f** zircon (Color figure online)

adsorption density generally increases with the increasing temperature for chemical types of adsorption. This phenomenon can be observed in Fig. 13 for the adsorption density values of all minerals with the exception of quartz.

The free energy of adsorption at 25 and 80 °C were calculated using the Stern–Grahame equation:

$$T_\delta = 2rC\exp\left(-\Delta G_{\text{ads}}^\circ / RT\right),$$

where T_δ is the adsorption density in the stern plane, r is the effective radius of the adsorbed ion, C is the equilibrium concentration, $\Delta G_{\text{ads}}^\circ$ is the standard adsorption free energy. Results are presented in Fig. 14.

Knowing the free energy at two different temperatures, the enthalpy and entropy were calculated by means of the following thermodynamic equations:

$$\Delta H_{ads}^{\circ} = \left[\left(\Delta G_1^{\circ}/T_1 \right) - \left(\Delta G_2^{\circ}/T_2 \right) \right] / \left(1/T_1 - 1/T_2 \right)$$

$$\Delta S_{ads}^{\circ} = \left(\Delta G_1^{\circ} - \Delta G_2^{\circ} \right) / \left(T_2 - T_1 \right)$$

Table 1 summarizes the thermodynamic results obtained from this study.

Thermodynamic values were calculated with the assumption that ΔH and ΔS are independent of temperature, in the temperature range of 25 to 80 °C. As a result, ΔG appears to be linearly related to temperature. In actuality, ΔG could experience nonlinear relationship at temperatures within this interval, which can generate different ΔH and ΔS values for different temperature ranges.

Experiments were conducted to evaluate the effect of pH on adsorption density. Figure 15 presents the adsorption density as a function of initial pH. The initial concentration, in this case, is 10^{-3} M of octanohydroxamic acid.

Ilmenite has the highest adsorption density over the entire range of pH used in this experiment with the exception of the interval from pH 8.5 to 10. In this interval, apatite has the highest adsorption with a peak at pH 9. The adsorption density of octanohydroxamic acid on the surfaces of monazite, rutile, zircon, and quartz shows a weak dependency of pH, as opposed to ilmenite and apatite. The adsorption density of ilmenite increases with the decreasing pH. This may be due to the increase of ferric ions that

occurs in more acidic environment [22]. Higher adsorption density of octanohydroxamic acid on ilmenite is due to higher stability constant of ferric hydroxamate [23]. Table 2 shows the stability constant of certain metal

Table 2 Stability constant for metal acetohydroxamate at 20 °C [24]

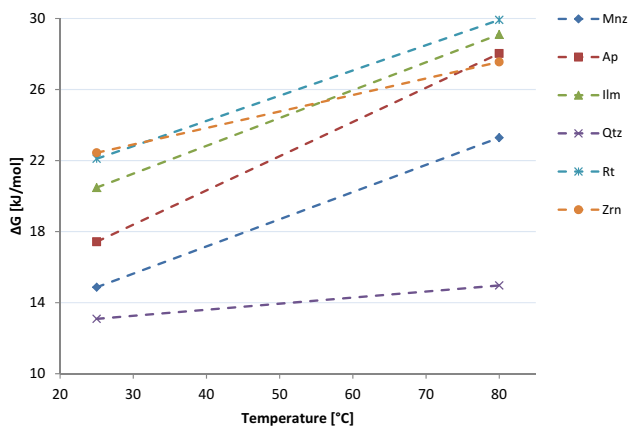| Cation	Log K_1	Log K_2	Log K_3
Ca^{2+}	2.4		
Mn^{2+}	4.0	2.9	
Cd^{2+}	4.5	3.3	
Fe^{2+}	4.8	3.7	
Co^{2+}	5.1	3.8	
Ni^{2+}	5.3	4.0	
Zn^{2+}	5.4	4.2	
Pb^{2+}	6.7	4.0	
Cu^{2+}	7.9		
La^{3+}	5.16	4.17	2.55
Ce^{3+}	5.45	4.34	3.0
Sm^{3+}	5.96	4.77	3.68
Gd^{3+}	6.10	4.76	3.07
Dy^{3+}	6.52	5.39	4.04
Yb^{3+}	6.61	5.59	4.29
Al^{3+}	7.95	7.34	6.18
Fe^{3+}	11.42	9.68	7.23

Fig. 14 Free energy of adsorption as a function of temperature
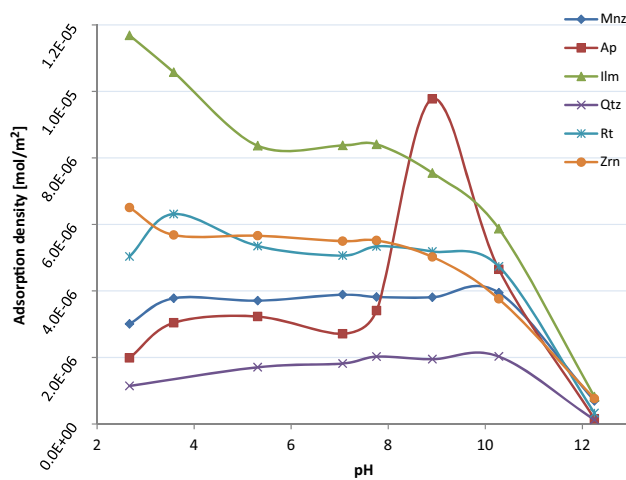
Fig. 15 Adsorption density as a function of pH

Table 1 Thermodynamic parameters of adsorption

Mineral	ΔG_{298} (kJ/mol)	ΔG_{353} (kJ/mol)	ΔH (kJ/mol)	ΔS (J/mol)
Monazite	−14.87	−23.29	30.75	153.08
Apatite	−17.43	−28.03	39.99	192.68
Ilmenite	−20.48	−29.1	26.22	156.72
Quartz	−13.09	−14.91	−2.9	34.19
Rutile	−22.10	−29.29	20.25	142.12
Zircon	−22.4	−27.5	5.67	92.97
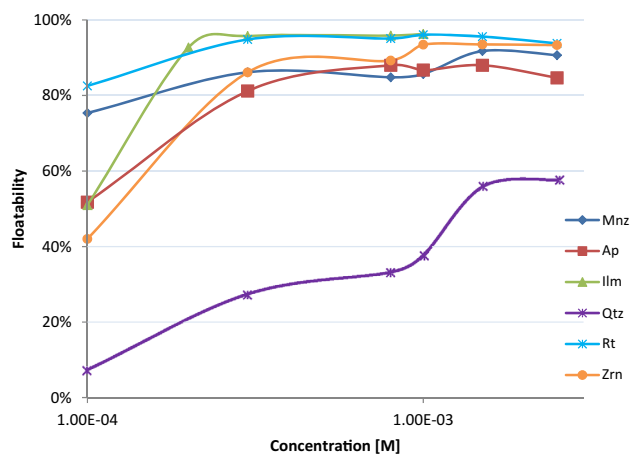
Fig. 16 Effect of concentration on floatability at 25 °C

Fig. 17 Effect of pH on floatability at initial concentration of 0.001 M octanohydroxamic acid

acetohydroxamate complexes at 20 °C [24]. It can be seen that trivalent complexes have higher stability constant, the strongest being that of iron.

At a higher pH value (12), the adsorption density decreases remarkably. This occurs above the pH value of dissociation of octanohydroxamate (9.5). The higher pH values yield octanohydroxamate anions. In addition, the increasing pH results in the increasing negative value of surface charge of minerals, as shown in the zeta potential measurements. The occurrences of these two phenomena together enhance the repulsive interaction between octanohydroxamate ions and negatively charged particles.

It is important to note that the effect of pH on adsorption was evaluated with 10^{-3} M of octanohydroxamic acid. Different concentrations could result in different behaviors in terms of pH dependency on adsorption. The combined effect of pH and concentration on adsorption was not within the scope of this study.

Microflotation

The first series of experiment aimed to determine the flotation response of each mineral as a function of collector concentration at their natural pH. The results are illustrated in Fig. 16.

The recovery rates of monazite, apatite, ilmenite, rutile, and zircon increase sharply at a low concentration range (10^{-4}–3×10^{-4} M). The recovery rate of quartz remains relatively low, and maximum recovery of 60% was at 2.5×10^{-3} M concentration of collector solution.

The effects of pH on the floatability were evaluated at concentrations of 2×10^{-4} and 10^{-3} M of octanohydroxamic acid. The results are plotted in Figs. 17 and 18, respectively.

At 0.001 M, the recovery rates of ilmenite, rutile, and zircon show little dependency on pH in the range of
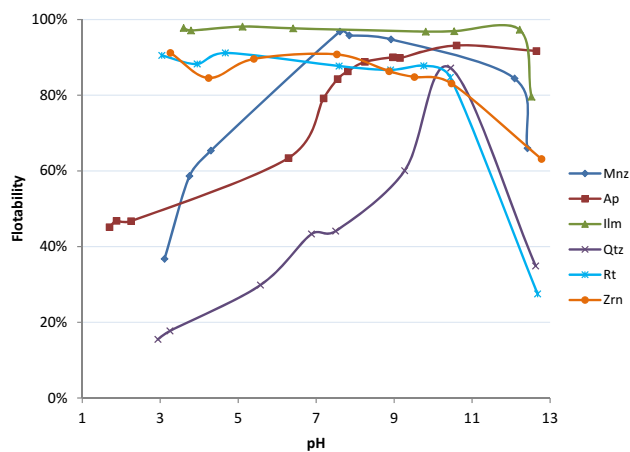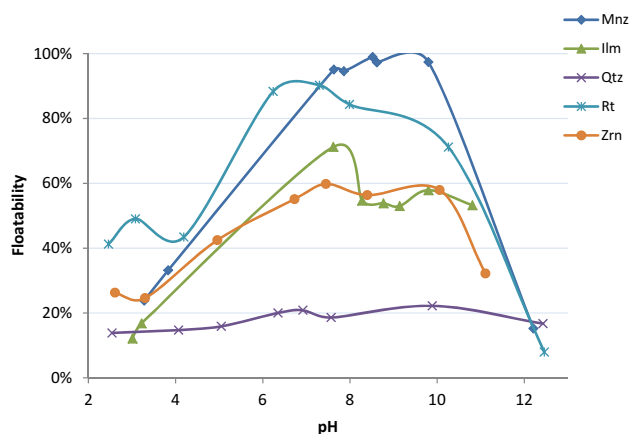

Fig. 18 Effect of pH on floatability at initial concentration of 0.0002 M octanohydroxamic acid

3.5–12. The recovery decreases sharply at higher pH values. Monazite shows maximum floatability at pH in the range of 7.5–10. Apatite floatability increases with the increasing pH; at 12.6, apatite has maximum floatability. Quartz has the lowest floatability with a peak at pH 10.4.

At 0.0002, the floatability values of ilmenite, rutile, and zircon decrease at acidic pH values. The floatability of monazite remains unchanged with a peak at pH 7.6–9.8. In this interval, monazite has the highest floatability. However, the difference is too negligible to allow for reasonable separation.

The effect of temperature was evaluated by conditioning at 80 °C. The results are shown in Fig. 19.

Similar to the result observed at room temperature, the floatability behaviors of monazite and associated minerals have parallel response with respect to temperature and collector concentration. Quartz, on the other hand, shows the lowest floatability, which is consistent with results obtained from adsorption density. One important point to
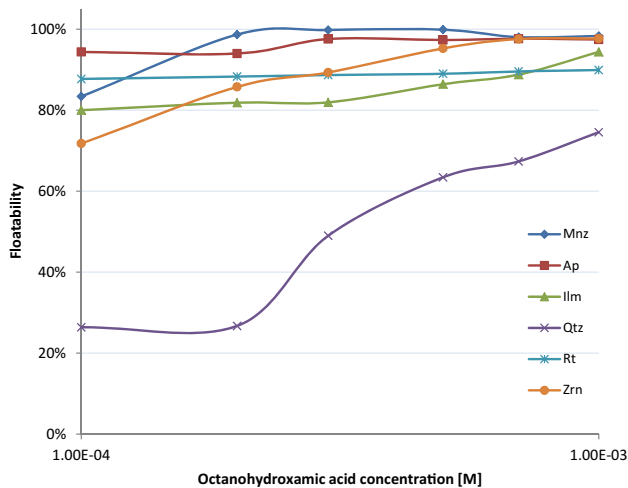
Fig. 19 Effect of concentration of octanohydroxamic acid on floatability at 80 °C

note is that the floatability at lower concentration (10^{-4} M of octanohydroxamic acid) increases when the temperature is increased to 80 °C.

Although ilmenite has the highest adsorption densities at both temperatures, its floatability is lower than those of monazite, apatite, rutile, and zircon. High adsorption may result in nearly total depletion of octanohydroxamic acid in the solution, which will decrease the froth, and thus decrease recovery.

The results obtained in microflotation experiments illustrate the flotation responses of minerals in different environments using octanohydroxamate acid as a collector. These results can be used as a basis of mineral separation and concentration in a system containing monazite and minerals investigated in this study. A bulk flotation test, however, may be complicated by the presence of various dissolved species in solution.

Conclusion

The IEP values of monazite, apatite, ilmenite, quartz, rutile, and zircon are 5.3, 8.7, 3.8, 3.4, 6.3, and 5.1, respectively. Addition of octanohydroxamic acid alters the zeta potential of minerals, due to interaction of collector molecules with lattice atoms. Octanohydroxamate acid adsorbs on the negatively charged solid minerals, which verifies that chemisorption takes place.

Adsorption density measurements show that octanohydroxamate acid adsorbs onto the surfaces of monazite and gangue minerals as well. At higher pH environments, adsorption decreases due to the electrostatic repulsion between hydroxamate anions and negatively charged surface. As seen in thermodynamic calculations, ilmenite has

higher affinity to hydroxamate due to higher stability constant of ferric hydroxamate.

Microflotation experiments confirm that the flotation response of monazite is very similar to that of its gangue minerals when using octanohydroxamic acid as a collector. Monazite is best recovered at a pH range of 7.5–10. A variation of the collector concentration alone is not sufficient to establish the separation of theses minerals.

The results obtained in this study provide a strong basis on the flotations of monazite, apatite, ilmenite, quartz, rutile, and zircon minerals with octanohydroxamic acid. This can be used as a foundation for the separation and the concentration of monazite from its associated minerals.

References

1. Pavez O, Peres AEC (1993) Flotation of monazite-zircon-rutile with sodium oleate and hydroxamates. In: XVII international mineral processing congress (Australasian Institution of Mining and Metallurgy, Sydney)
2. Ren J, Song S, Lopez-Valdivieso A, Li S (1999) Selective flotation of bastnaesite from monazite in rare earth concentrates using potassium alum as depressant. Int J Miner Process 59:237–245. doi:10.1016/S0301-7516(99)00075-7
3. McEwen R, Hansen G, Lee G (1976) Single stage flotation of alkali feldspars, ilmenite, rutile, garnet, and monazite, with mixed cationic/anionic collectors. Transactions 260:97–100
4. Abeidu AM (1972) The separation of monazite from zircon by flotation. J Less Common Metals 29(113–119):1016. doi:10.1016/0022-5088(72)90181-6
5. Cheng TW (1999) The point of zero charge of monazite and xenotime. Miner Eng 13:105–109. doi:10.1016/S0892-6875(99)00153-3
6. Viswanathan et al (1965) Selective flotation of beach sand monazite. Min Mag 113(1):17–23
7. Zakharov E, Pol'kin I, Ilie P, Solnyshkin VI (1967) Selective desorption of sodium oleate from pyrochlore, zircon, and monazite by sodium sulfide. In: Plaksin IN (ed) Paper from flotation properties of rare earth metal mineral. Primary Sources, New York, pp 46–56
8. Pavez O, Brandao P, Peres A (1995) Adsorption of oleate and octyl-hydroxamate on to rare-earths minerals. Miner Eng 9(3):357–366. doi:10.1016/0892-6875(96)00020-9
9. Raghavan S, Fuerstenau DW (1974) The adsorption of aqueous octylhydroxamate on ferric oxide. J. Colloid Interface Sci 50(2):319–330. doi:10.1016/0021-9797(75)90235-0
10. Pradip. K (1981) Surface properties and flotation of rare earth minerals. PhD thesis, University of California, Berkeley
11. Grahame DC (1947) The electrical double layer and the theory of capillarity. Chem Rev 41:441–501. doi:10.1021/cr60130a002
12. Pavez O, Peres AEC (1992) Effect of sodium metasilicate and sodium sulphide on the floatability of monazite-zircon-rutile with oleate and hydroxamates. Miner Eng 6:69–78. doi:10.1016/0892-6875(93)90164-I
13. Houot R, Cuif J, Mottot Y, Samama J (1991) Recovery of rare earth minerals with emphasis on flotation process. In:

Proceedings of international conference on rare earth minerals and minerals for electronic uses, Hat Yai, pp. 301–324

14. Mishra SK (1977) The electrokinetics of apatite and calcite in inorganic electrolyte environment. Int J Miner Process 5:69–83. doi:10.1016/0301-7516(78)90006-6

15. Zhou F, Wang L, Xu Z, Liu Q, Chi R (2014) Reactive oily bubble technology for flotation of apatite, dolomite and quartz. Int J Miner Process 134:74–81. doi:10.1016/j.minpro.2014.11009

16. Amankonah JO, Somasundaran P (1985) Effects of dissolved mineral species on the electrokinetic behavior of calcite and apatite. Colloid Surf 15:335–353. doi:10.1016/0166-6622(85)80082-2

17. Mehdilo A, Irannajad M, Rezai B (2013) Effect of chemical composition and crystal chemistry on the zeta potential of ilmenite. Colloids Surf A 428:111–119. doi:10.1016/j.colsurfa.2013.03.032

18. Zhou Y, Zhang Y, Li G, Wu Y, Jiang T (2014) A further study on adsorption interaction of humic acid on natural magnetite, hematite and quartz in iron pelletizing process: effect of the solution pH value. Powder Technol 271:155–156. doi:10.1016/j.powtec.2014.10.045

19. Somasundara P, Ofori-Amankonah J, Ananthapadmabhan. KP (1985) Mineral-solution equilibria in sparingly soluble mineral system. Colloid Surf 15:309–333. doi:10.1016/0166-6622(85)80081-0

20. Siivola J, Schimd R (2007) List of minerals abbreviation. https://www.bgs.ac.uk/scmr/docs/papers/paper_12.pdf. Accessed 1 Dec 2016

21. Chander S, Fuerstenau DW (1975) Electrochemical reaction control of contact angles on copper and synthetic chalcocite in aqueous potassium diethyldithiophosphate solutions. Int J Miner Process 2:333–352. doi:10.1016/0301-7516(75)90027-7

22. Fuerstenau C, Harper R, Miller J (1970) Hydroxamate versus fatty acid flotation of iron oxide. Soc Min Eng AIME 247:69–73

23. Fuerstenau MC (2005) Chelating agents as flotation collectors. Innovation in natural resource processing. SME Publication, Littleton, pp 33–56

24. Schwartzenbach G, Schwartzebach K (1963) Hydroxamate komplexes. Diestabilitat der eisen (III) – konplexe einfacher hydroxamsauren und der ferrioxamins B. Helv Chim Acta 46:1403